

IN VIVO FLUORESCENCE AND REFLECTANCE IMAGING OF HUMAN CERVICAL TISSUE

Ulf Gustafsson, Elisabeth McLaughlin, Ellen Jacobson,
Johan Håkansson, Paul Troy and Michael DeWeert
Science and Technology International[®], 733 Bishop Street, Suite 3100,
Honolulu, Hawaii 96813, USA

Sara Pålsson, Marcelo Soto Thompson, and Sune Svanberg
*Lund Institute of Technology, Department of Physics, P.O. Box 118,
SE-221 00 Lund, Sweden*

Aurelija Vaitkuvienė
*Vilnius University Hospital, Department of Obstetrics and Gynecology,
Antakalnio str. 57, 2040-LT, Vilnius, Lithuania*

Katarina Svanberg
*Lund University Hospital, Department of Oncology,
SE-221 85 Lund, Sweden*

ABSTRACT

A hyperspectral imaging spectrograph has been used to measure the fluorescence and reflectance of cervical tissue *in vivo*. The instrument was employed in a clinical trial in Vilnius, Lithuania, where 111 patients were examined. The patients were initially screened by Pap smear, examined by colposcopy and a tissue sampling procedure was performed. Detailed histopathological assessments were performed on the biopsies, and these assessments were correlated with spectra and images. The results of the spectroscopic investigations show that different tissue types within one biopsy region exhibit different spectral signatures. A spectral analysis of the entire image localizes dysplastic regions in both fluorescence and reflectance, suggesting that the hyperspectral imaging technique is useful in the management of cervical malignancies.

Keywords: Fluorescence spectroscopy, reflectance spectroscopy, hyperspectral imaging, cervical intraepithelial neoplasia, malignancy detection.

1. Introduction

Tissue fluorescence and reflectance are promising diagnostic tools for the identification of early cervical malignancies [1-6]. During recent years several spectroscopic and imaging techniques for early cervical malignancy detection have been developed. Systems based on point monitoring and fiber optic probes are simple but have proven efficient in many studies. However, imaging spectroscopy simultaneously providing spectral information on a whole investigated scene has clear advantages in many clinical settings. Imaging spectroscopy is particularly interesting for applications where the borders of the malignancies cannot easily be visualized by the naked eye, e.g. in the female outer gynecological tract, the pulmonary and ENT regions. Recent overviews of medical fluorescence imaging are given in, e.g., Refs. 7 and 8.

In the development of new diagnostic techniques, classical histopathology clearly is the gold standard to be applied for correlation with the new data. A problem using the standard histopathological protocol is that only the most severe finding of the studied region is reported. Imaging spectroscopy will, on the other hand, provide thousands of individual tissue spectra characterizing all parts of the investigated tissue area. To overcome this problem, a detailed histopathological protocol was introduced [9]. This protocol allows for the correlation of the fluorescence and reflectance spectra with the actual biological status of the area studied and provides a histopathological map to match the hyperspectral images. In this way, data from the clinical trial could be efficiently utilized.

The most widely used method for initial screening for cervical intraepithelial neoplasia (CIN) and cervical cancer is a cytological smear. A 20 to 30 % false negative rate is associated with the Papanicolaou (Pap) smear due to insufficient sampling of cells and also to the fact that the technique is based on exfoliated cells which biological status can be misinterpreted [10]. Estimates of the sensitivity and specificity of Pap smears have been shown to range from 11 - 99% and 14 - 97%, respectively [11]. An abnormal Pap smear is normally followed by colposcopy, biopsy, histological evaluation and diagnosis. The diagnostic procedure often also includes a human papilloma virus (HPV) test for classification of the various classes of HPV. Colposcopy is performed in cases with positive results for high-risk HPV and if there is an identified lesion. The outcome of colposcopy in terms of differentiating between cervical intraepithelial lesions of various grades (CIN I-III) and inflammation/infection is highly variable and limited by operator expertise. In experienced hands, the performance average for colposcopy is sensitivity of $94 \pm 14\%$, a specificity of $51 \pm 24\%$ and a positive predictive value of $83 \pm 15\%$ [12]. In order to improve the objectivity of cervical cancer screening, tissue fluorescence and reflectance spectroscopy have been suggested as a viable diagnostic aid to the physician to demarcate premalignant lesions and to guide the biopsy procedure. Different groups are currently developing suitable technology [2-4,13].

We have performed an extensive study aiming at evaluating the potential of a novel hyperspectral diagnostic imaging (HSDI®) instrument, designed and built by Science and Technology International®. The study was performed at the Vilnius University Hospital, Lithuania. The investigation was supported by recordings from a point monitoring fluorescence spectroscopy device developed by the Lund Institute of Technology.

The clinical study provided a very large amount of useful data. The data are now being evaluated but as a preview, preliminary results are presented in this paper. A companion paper [14] gives an example of the image-processing aspects of the problem, which is greatly facilitated by the detailed histopathology of the excised tissue samples.

2. Methods and Patients

2.1. *Hyperspectral diagnostic imaging instrument*

The HSDI instrument is a hyperspectral imaging spectrograph for early diagnosis of cervical malignancy; see Figure 1. The instrument combines reflectance and fluorescence capabilities and collects white light reflectance and fluorescence hyperspectral images in the 400 to 760 nm region. The spatial resolution of the instrument is 230 microns at the normal working distance of 0.3 meters. The instrument includes also a high-resolution digital RGB camera, which is used to collect standard colposcopic images concurrently with hyperspectral imaging. The RGB images are used as references for registering the fluorescence and reflectance, and for marking the localization of collected biopsy specimen.



Figure 1. The Hyperspectral Diagnostic Imaging instrument in the clinical setting in Vilnius.

2.2. Hyperspectral imaging

Hyperspectral imaging is characterized by the generation of a hyperspectral cube that contains spatial information in two dimensions and spectral information in the third dimension. The hyperspectral data collection procedure of the HSDI instrument is outlined in Figure 2. The hyperspectral sensor uses a progressive line scan to capture an entire image. Figure 2a shows the conventional colposcopic RGB image. For each scan line, the full spectrum for every pixel is provided, as indicated in Figure 2b. By taking a number of lines, a hyperspectral cube is developed, shown in Figure 2c. The HSDI hyperspectral data cube consists of about 30,000 image points with full spectral information. The hyperspectral cubes are spectrally and spatially corrected for the spectral and spatial non-uniformity of the optics, detectors and illumination sources using a reflectance standard and an integrating sphere, both NIST-calibrated.

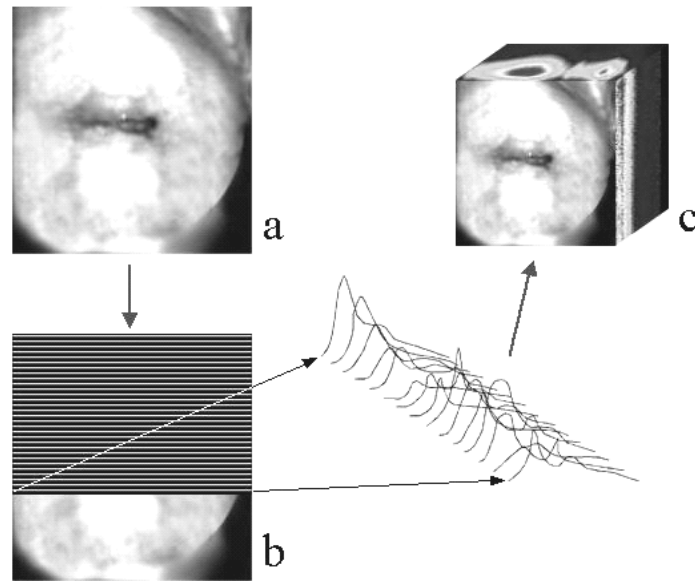


Figure 2. The line scan procedure used in the HSDI instrument. a) Conventional colposcopic image. b) Line scan with associated spectrum for each pixel. c) Resulting hyperspectral cube.

2.3. Clinical set-up

The clinical study was conducted in Vilnius, Lithuania, and patients for the study consisted of postmenarchal women with indications for colposcopy. Women were recruited to undergo hyperspectral imaging and point monitoring measurements during their colposcopic examination. Inclusion criteria were females over the age of 18, indication for colposcopy or due for routine pelvic examination, no history of cervical dysplasia, and no acute diagnosis of infectious cervicovaginitis. Patients were excluded if they had a known or suspected pregnancy. One hundred eleven patients were enrolled in the study, which was approved by the Lithuanian bioethics committee.

After obtaining informed consent, the patient's demographic data and pertinent medical history were gathered. The patients were placed in the examination position and a vaginal speculum was inserted. The HSDI instrument was positioned to optimize the focus of the instrument. The cervix was first scanned in a reflectance recording with white light for approximately 10 seconds. This was followed by a fluorescence scan, requiring approximately 12 seconds. Both the fluorescence and the reflectance scans are non-contact and non-invasive. Concomitantly with the hyperspectral image scans, standard colposcopic images were collected.

Following the two scans the cervix was cleansed with a large cotton swab soaked with a diluted solution (3-5%) of acetic acid as is standard practice in colposcopy. After application of acetic acid, the epithelium is whitened due to the dissolution of the mucus, and intracellular dehydration and coagulation of proteins. The patterns that appear, punctuation, mosaic structures and atypical vessels, are identified by the gynecologist. These signs are, however, seen in both pre-cancerous lesions and various degrees of cervicitis. The clinical challenge is, thus, to find a tool to discriminate between these conditions. A colposcopic examination of the cervix according to the standard procedure was conducted using white light illumination. The physician inspected the cervix for lesions and areas of suspicion. This was followed by "post-acetic" reflectance and fluorescence scans as well as standard colposcopic images. Based on the colposcopic findings, biopsies, sections, mini-, and maxi-conizations were taken using electrical loops.

Examples of reflectance and fluorescence images acquired before and after the application of acetic acid are shown in Figure 3. The atypical areas are clearly visible in the post-acetic reflectance image as aceto-whitened regions. These regions are not as obvious in the post-acetic fluorescence image.

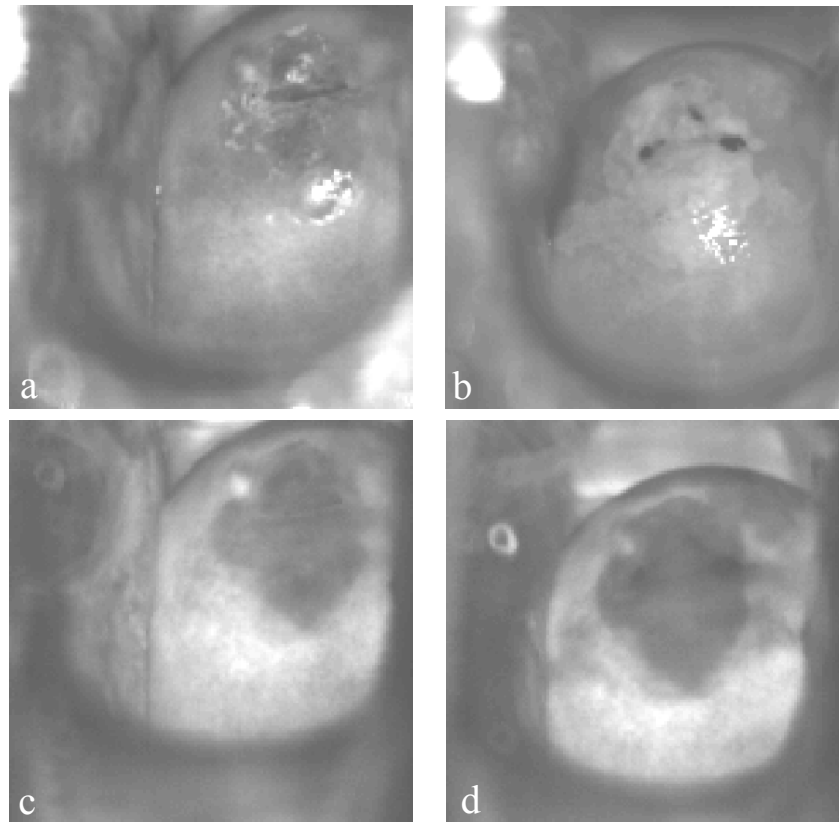


Figure 3 a-b) Reflectance images from one wavelength band in the hyperspectral reflectance cube. c-d) Fluorescence images from one wavelength band in the hyperspectral fluorescence cube. Images a and c are acquired before the application of acetic acid and images b and d are acquired after the application.

2.4. Histopathology

Excised tissue samples were prepared for pathologic examination. Two independent pathologists reviewed the micrographic slides. The first pathology examination was conducted in Vilnius and the result was immediately reported to the patient and used for treatment and follow-up. A pathologist in Lund, Sweden, conducted a second pathology review. This review was performed according to the detailed histopathological protocol [7] and accounted for multiple sites and morphological details potentially influencing the spectrum recorded. The orientation and location of the biopsy sites were recorded as precisely as possible on sampling. The examination allowed for a very accurate correlation between histopathology and the optical signals. Figure 4 shows an example of biopsy sites and pathological information according to the new detailed protocol. The new protocol clearly demarcates acetic acid whitened pre-cancerous lesions and other atypical regions although not pre-cancer. The histopathological examination revealed a lesion, moderate grade dysplasia (CIN II), in middle section of biopsy region 1.

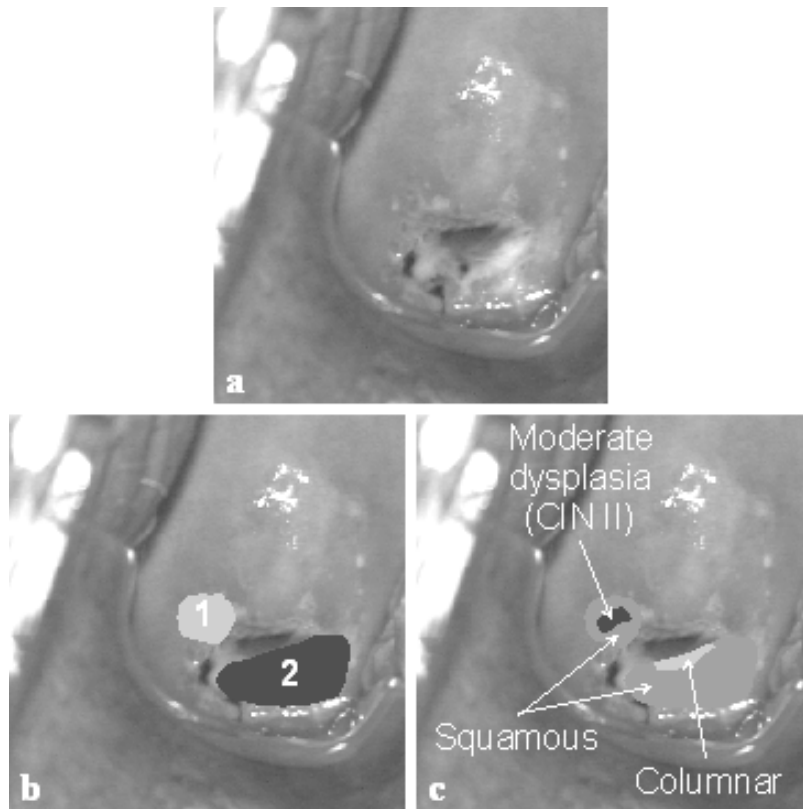


Figure 4. Examples of a reflectance image (a), geometrically referenced biopsies (b) and classified tissue types (c).

3.Results

Using the detailed pathology method, the opportunities are given to construct histopathology maps of the cervical area and to correlate each individual recorded spectrum with the detailed pathology evaluated in the corresponding region. Full hyperspectral reflectance and fluorescence image cubes as well as RGB color images were acquired for all of the patients. The biopsied regions were indicated on the reflectance image for correlation with the histopathological examination. The RGB image, the biopsy sites and the histopathological map for the patient data shown in Figure 3 are presented in Figure 5. According to the histopathological examination, high-grade dysplasia (CIN III) is present close to the cervical channel. Most of the regions biopsied were, however, diagnosed as normal squamous tissue.

The spectral signature in both reflectance and fluorescence from the different tissue regions are displayed in Figure 6. The spectra shown are the average spectra, and the average squamous spectra are taken from the three different biopsy regions. An overall intensity reduction in the dysplastic spectra, which is a common observation for malignancies (see, e.g., [15]), can be observed. Dysplastic regions tend to have an increased metabolism and larger blood flow than normal tissue, and the intensity reduction can be attributed to absorption of the white light in reflectance and re-absorption of the fluorescence light by oxy-hemoglobin. Hemoglobin in blood is strong absorber in the visible region, which also explains the fact that blood has the lowest intensity in both reflectance and fluorescence. The strong absorption bands of oxy-hemoglobin at 414 nm, 542 nm and 577 nm are clearly discernable in the reflectance spectra.

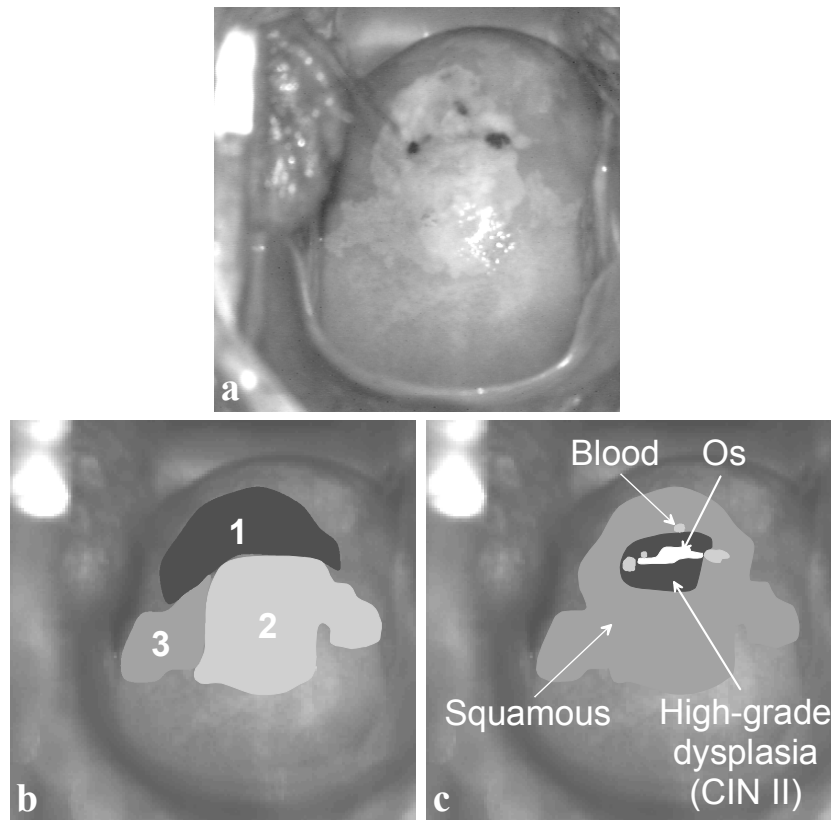


Figure 5 a) RGB image. b) Biopsied regions. c) Histopathological map.

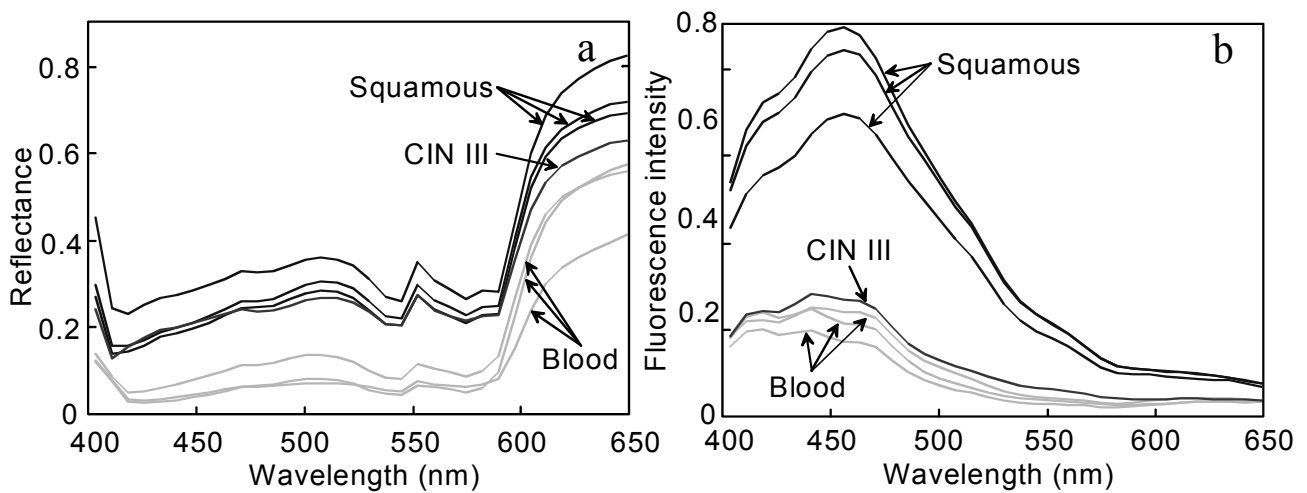


Figure 6 Average reflectance (a) and fluorescence (b) spectra from squamous tissue, high-grade dysplasia (CIN III) and blood.

A spectral analysis using Bayesian multi-variant statistics of the reflectance and the fluorescence hyperspectral images is shown in Figure 7. Detections for high-grade dysplasia are localized in the region of the lesion in both reflectance and fluorescence.

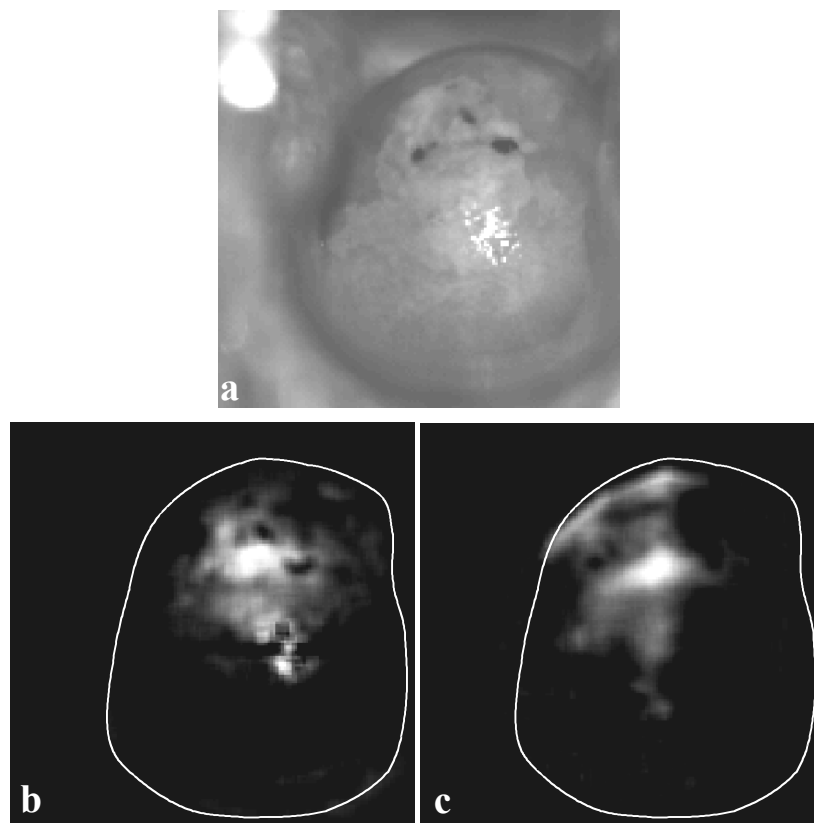


Figure 7 Spectral analysis of the reflectance and the fluorescence hyperspectral image cubes. a) Reflectance image of the cervix. b-c) Corresponding spectral detection of moderate grade dysplasia (CIN II) in reflectance and fluorescence, respectively.

Figure 8 displays the spectral analysis of the hyperspectral images from a patient with moderate grade dysplasia (see Figure 4). Detections for moderate dysplasia are for this patient also localized in the region of the lesion in both reflectance and fluorescence. For both examples shown here, detection is also visible in other, aceto-whitened, regions on the cervix. These regions were, however, not biopsied.

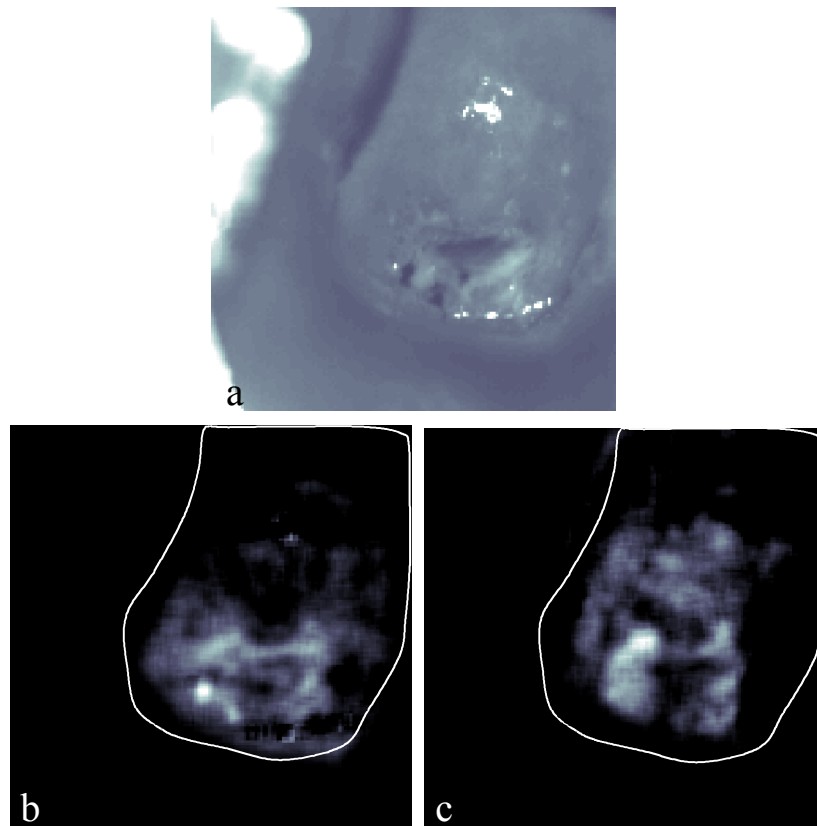


Figure 8. Spectral analysis of the reflectance and the fluorescence hyperspectral image cubes. a) Reflectance image of the cervix. b-c) Corresponding spectral detection of low/moderate grade dysplasia in reflectance and fluorescence, respectively.

4. Discussion and conclusions

We have employed a hyperspectral imaging instrument in a clinical study to evaluate the potential of the instrument for the detection of early cervical malignancies. In this paper we have presented preliminary results of this work. The very large amount of data collected during the clinical trial is now being evaluated and will be presented in a future paper.

The analysis utilized a new detailed histopathological protocol which accounts for multiple sites and provides a detailed histopathological map within the regions biopsied. The new histopathological examination allows for a very accurate correlation between histopathology and the recorded spectral signal. This correlation is illustrated in Figure 6, where different tissue types within biopsy regions exhibit different spectral signatures. Compared to squamous tissue, an overall intensity reduction is observed in the dysplastic spectra. This correlation would not be possible using the standard histopathological protocol, which only reports the most severe condition within the entire biopsy region.

A spectral analysis of the entire image detects, as illustrated in Figure 7 and Figure 8, the moderate and high-grade dysplastic lesions in both fluorescence and reflectance. Suspected false alarm lesions can also be identified. Most of these regions were, however, not biopsied, making it difficult to determine whether they are true false alarms. Histopathological information is only available within the excised tissue regions, and it is only within these regions a true correlation between the histopathological map and the spectral signatures can be made. An advantage of spectral imaging, as compared to point monitoring systems, is the generation of a hyperspectral image cube with a very large number of spectra available for processing. This information can be used to guide the physician to other suspicious tissue regions.

ACKNOWLEDGMENTS

The authors would like to recognize Jody Oyama and R.B. Sieple for operating the HSDI instrument during the clinical trials, and Reda Ziobakiene, Violeta Poskiene, and Kristina Kriukelyte for performing Vilnius clinical trial colposcopy examinations and biopsy sampling. The authors are further grateful to Unne Stenram for detailed histopathological work, Gary Bignami and Stefan Andersson-Engels for insightful discussions on medical spectroscopy, and Nicolas Susner and Science and Technology International for supporting this work.

REFERENCES

1. S. Andersson-Engels, Å. Elner, J. Johansson, S.-E. Karlsson, L.G. Salford, L.-G. Strömblad, K. Svanberg and S. Svanberg, Clinical recording of laser-induced fluorescence spectra for evaluation of tumour demarcation feasibility in selected clinical specialities, *Lasers Med. Sci.* **6**, 415-424 (1991).
2. R.J. Nordstrom, L. Burke, J.M. Niloff and J.F. Myrtle, Identification of cervical intraepithelial neoplasia (CIN) using UV-excited fluorescence and diffuse-reflectance tissue spectroscopy, *Lasers Surg. Med.* **29**, 118-127 (2001).
3. M.F. Mitchell, S.B. Cantor, N. Ramanujam, G. Tortolero-Luna and R. Richards-Kortum, Fluorescence spectroscopy for diagnosis of squamous intraepithelial lesions of the cervix, *Obstet. Gynecol.* **93**, 462-470 (1999).
4. I. Georgakoudi, E.E. Sheets, M.G. Müller, V. Backman, C.P. Crum, K. Badizadegan, R.R. Dasari, and M.S. Feld, Trimodal spectroscopy for the detection and characterization of cervical precancers in vivo, *Am. J. Obstet. Gynecol.* **186**, 374-382 (2002).
5. Y.N. Mirabal, S.K. Chang, E.N. Atkinson, A. Malpica, M. Follen, and R. Richards-Kortum, Reflectance spectroscopy for in vivo detection of cervical precancer, *J. Biomed. Opt.* **7**, 587-594 (2002).
6. C. af Klinteberg, M. Andreasson, O. Sandström, S. Andersson-Engels and S. Svanberg, Compact medical fluorosensor for minimally invasive tissue characterisation, Submitted to *Rev. Sci. Instrum.* (2002).
7. G.A. Wagniers, W.M. Star, and B.C. Wilson, In vivo fluorescence spectroscopy and imaging for oncological applications, *Photochem. Photobiol.* **65**, 603-632 (1998).
8. S. Andersson-Engels, K. Svanberg and S. Svanberg, Fluorescence imaging in medical diagnostics, in *Biomedical Optics*, ed. J.G. Fujimoto, to appear.
9. S. Pålsson, U. Stenram, M. Soto Thompson, A. Vaitkuviene, V. Poskiene, R. Ziobakiene, J. Oyama, N. Bendsoe, S. Andersson-Engels, S. Svanberg and K. Svanberg, Methods for detailed histopathological investigation and localisation of cervical biopsies to improve the interpretation of autofluorescence data, Manuscript in preparation (2003).
10. L.G. Koss, The Papanicolaou test for cervical cancer detection: A triumph and tragedy, *JAMA* **261**, 737-743 (1989).
11. M.T. Fahey, L. Irwig, and P. Macaskill, Metaanalysis of pap test accuracy, *Am. J. Epidemiol.* **141**, 680-689 (1995).
12. M.F. Mitchell, Accuracy of colposcopy, *Consult. Obstet. Gynecol.* **6**, 70-73 (1994).
13. C. af Klinteberg, C. Lindquist, I. Wang-Nordman, A. Vaitkuviene and K. Svanberg, Laser-induced fluorescence studies of premalignant and benign lesions in the female genital tract, in *Optical Biopsies and Microscopic Techniques II*, eds. I.J. Bigio, K. Svanberg, H. Schneckenburger, J. Slavik and P.M. Viallet, *Proc. SPIE* vol. **3197**, 34-40 (1997).
14. M.J. DeWeert, J. Oyama, E. McLaughlin, E. Jacobson, J. Håkansson, G.S. Bignami, U. Gustafsson, P. Troy, V. Poskiene, K. Kriukelyte, R. Ziobakiene, A. Vaitkuviene S. Pålsson, M.S. Thompson, U. Stenram, S. Andersson-Engels, S. Svanberg, and K. Svanberg, Analysis of Spatial Variability in Hyperspectral Imagery of the Uterine Cervix In Vivo, in *Spectral Imaging: Instrumentation, Applications and Analysis*, eds. R.M. Levenson, G.H. Bearman, and A. Mahadevan-Jensen, *Proc SPIE* vol. **4959** (2003).
15. L. Baert, R. Berg, B. van Damme, M.A. D'Hallewin, J. Johansson, K. Svanberg and S. Svanberg, Clinical fluorescence diagnosis of human bladder carcinoma following low-dose Photofrin injection, *Urology* **41**, 322-330 (1993).